Acta Crystallographica Section A
Foundations of Crystallography
ISSN 0108-7673

Received 16 March 2004
Accepted 20 April 2004

A Fourier optics approach to the dynamical theory of X-ray diffraction – continuously deformed crystals

Giovanni Mana[a]* and Carlo Palmisano[b]

[a]CNR – Istituto di Metrologia 'G. Colonnetti', str. delle cacce 73, 10135 Torino, Italy, and [b]Università di Torino, Dipartimento di Fisica Generale 'A. Avogadro', v. P. Giuria 1, 10125 Torino, Italy. Correspondence e-mail: g.mana@imgc.cnr.it

X-ray diffraction in continuously deformed crystals is considered by application of Fourier optics and from the viewpoint of the analogy between X-ray dynamics and the motion of two-level systems in quantum mechanics. Different forms of Takagi's equations are traced back to a common framework and it is shown that they are different ways to represent the same propagation equation. A novel way to solve Takagi's equations in the presence of a constant strain gradient is presented and approximation methods derived from quantum mechanics are considered. Crystal deformation in X-ray interferometry and two-crystal spectrometry are discussed and it is demonstrated that Si lattice-parameter measurements depend on the diffracting plane spacing on the crystal surface.

1. Introduction

Our work was prompted by advances in the measurement of the Si lattice parameter by X-ray interferometry (Bonse & Hart, 1965; Bergamin *et al.*, 1999) and by two-crystal spectrometry (Hart, 1969; Kessler *et al.*, 1994). The sensitivity and accuracy of these techniques now require a detailed theoretical framework that includes the study of lattice deformation. Experimental evidence of anomalies was reported by Kessler *et al.* (1999) and Deslattes *et al.* (1999) and we collected indications that deformations may influence measurements in an unexpected way (Mana *et al.*, 2004*a*). In order to provide solid foundations to our investigations, a previous article (Mana & Montanari, 2004) gave a reformulation of the dynamical theory of X-ray diffraction based on Takagi's equations and Fourier optics. This reformulation extends the coupled pendulum model of dynamical diffraction (Ewald, 1965; Shevchenko & Pobydaylo, 2003) and makes extensive use of the analogy between the X-ray dynamics in crystals and two-level systems in quantum mechanics (Kato, 1973). The purpose of this article is to complete that reformulation by extending it to continuously deformed crystals.

In a perfect crystal, in the two-wave approximation of the dynamical theory, two propagation modes (in Ewald's terminology, wavefields) exist, any of which consists of a linear superposition of two plane waves whose wavevectors fall into continuous bands separated by a forbidden gap (Authier, 2001). These wavefields are the analogue of energy eigenstates of relativistic electrons and two-level atoms. In deformed crystals, as in their quantum-mechanical counterparts, perturbation of the Hamiltonian induces intra- and inter-branch transitions between perfect-crystal wavefields. In the general case, Takagi's equations have no analytical solutions and it is necessary to integrate them numerically. Yet numerical integration does not give a description of the underlying physics. However, if one takes into account that Takagi's equations have the same structure as Schrödinger's equation, more precisely as Dirac's equation, since both are linear in the derivatives, quantum mechanics (Fano, 1971) offers an additional viewpoint and the possibility of examining the relevant physics. Conversely, in a didactic perspective, the dynamical theory of X-ray diffraction could represent a model of quantum electrodynamics.

In §2, we trace the theory variants back to a common framework and we show that they are only different ways to represent the same equation. In §3, we examine in detail approximation methods and the relevant validity limits. In order to illustrate our formalism, in §4, we investigate a number of example deformations, including the uniform strain gradient for which an analytical solution is possible. In §5, we discuss the implications of our results in X-ray interferometry and in two-crystal spectrometry and demonstrate that Si lattice-parameter measurements depend on the diffracting plane spacing on the crystal surface. In Appendix *A*, we give a reasonable explanation for the effectiveness of substituting mathematical planes for the real crystal surface. The list of the main symbols we use is given in Appendix *B*.

2. Representation of Takagi's equations

Our analysis will be restricted to a semi-infinite symmetrically cut crystal occupying the $z \geq 0$ region and to a coplanar Laue reflection, where the normal to the crystal surface z lies in the reflection plane and the $z < 0$ region is a vacuum. Consequently, only two coordinates are involved and X-ray

diffraction is two-dimensional. This restriction does not cause loss of generality; the way to reduce a non-coplanar asymmetrical reflection to two dimensions is given by Mana & Montanari (2004). The crystal deformation is described by the strain field $\mathbf{u}(\mathbf{r})$, where $\mathbf{r} = x\hat{\mathbf{x}} + z\hat{\mathbf{z}}$ is a two-dimensional position vector. Since electric susceptibility is

$$\chi(\mathbf{r}) = \sum_{\mathbf{h}_0} \chi_{h0} \exp[-\mathrm{i}\mathbf{h}_0(\mathbf{r} - \mathbf{u})], \tag{1}$$

where $\mathbf{h}_0$ is any reciprocal vector in the absence of the deformation, we can define a locally perfect crystal whose generic reciprocal vector will be indicated by $\mathbf{h}$. By expanding $\mathbf{h}_0[\mathbf{r} - \mathbf{u}(\mathbf{r})]$ in series, we can prove that $\mathbf{h} = \mathbf{h}_0 - \nabla(\mathbf{h}_0\mathbf{u})$. Eventually, we indicate the reciprocal vector of the unstrained diffracting planes by $\mathbf{g}_0$, direct the x axis along $-\mathbf{g}_0$ and assume that the diffracting planes are symmetrical with respect to the origin, so that $\chi_g = \chi_{\bar{g}}$.

In the two-wave approximation of the dynamical theory of X-ray diffraction in crystals, the field states $|D(z)\rangle$ form the Hilbert space $\mathrm{c}^2 \otimes \mathcal{L}^2(\mathrm{R})$, where c^2 is a two-dimensional complex vector space (the space of the dispersion-surface branches) and $\mathcal{L}^2(\mathrm{R})$ is a space of square-integrable complex functions (the space of field amplitudes in the observation plane z = constant). The various forms of Takagi's equations are different ways of representing the abstract equation

$$\mathrm{i}\partial_z|D(z)\rangle = \mathbf{H}|D(z)\rangle, \tag{2}$$

where we use the Dirac bra/ket notation (Fano, 1971) and z is the evolution parameter. Throughout this paper, we shall use a two-component spinor-like representation of c^2. The linear operators in $\mathrm{c}^2 \otimes \mathcal{L}^2(\mathrm{R})$ are indicated by bold letters. Their direct- and reciprocal-space representations are matrices of infinite rank, *e.g.* $\delta(x - x')H(x; z)$ and $\widetilde{H}(q - q'; z)$, where q is conjugate to x and H and $\widetilde{H}$ are 2×2 complex matrices. Consequently, the operation of, say, $\mathbf{H}$ on $|D(z)\rangle$ implies the sum on the repeated c^2 index and the integration over the $\mathcal{L}^2(\mathrm{R})$ variable. By transforming the $|D(z)\rangle$ state according to $|\varphi(z)\rangle = \mathbf{W}(z)|D(z)\rangle$, where $\mathbf{W}$ is any non-singular operator, we obtain different explicit theory formulations. The transformed equation is

$$\mathrm{i}\partial_z|\varphi(z)\rangle = [\mathbf{W}\mathbf{H}\mathbf{W}^{-1} - \mathrm{i}\mathbf{W}(\partial_z\mathbf{W}^{-1})]|\varphi(z)\rangle. \tag{3}$$

In the study of X-ray propagation, the evolution operator $\mathbf{U}(z)$ is determined, by means of which the initial field state $|D(0)\rangle$ is translated, that is, $|D(z)\rangle = \mathbf{U}(z)|D(0)\rangle$. Its reciprocal-space representation, $\widetilde{U}(q, q'; z) = \langle q|\mathbf{U}(z)|q'\rangle$ is called the optical transfer matrix. In the case of a perfect crystal, the transfer matrix is diagonal and will here be indicated by $\delta(q - q')\widetilde{U}_0(q, z)$.

2.1. *O–G* representation

The *O–G* representation of the crystal field,

$$\mathbf{D}(\mathbf{r}) = [D_O(\mathbf{r})\exp(-\mathrm{i}\mathbf{K}_O\mathbf{r})\hat{\mathbf{e}}_O + D_G(\mathbf{r})\exp(-\mathrm{i}\mathbf{K}_G\mathbf{r})\hat{\mathbf{e}}_G] \times \exp(-\mathrm{i}\kappa z), \tag{4}$$

where the σ and π subscripts indicating polarization are omitted and $\hat{\mathbf{e}}_O$ and $\hat{\mathbf{e}}_G$ are unit vectors orthogonal (σ polarization) or parallel (π polarization) to the (x, z) plane, uses the plane waves $\langle\mathbf{r}|n\rangle = \exp(-\mathrm{i}\mathbf{K}_n\mathbf{r})$, where $n = O, G$ and $|n\rangle \in \mathrm{c}^2$, as the basis functions. The field amplitudes $D_n(x; z) = \langle x|D_n(z)\rangle$ and $\widetilde{D}_n(q; z) = \langle q|D_n(z)\rangle$, where $\langle x|q\rangle = \exp(-\mathrm{i}qx)$, are the direct- and reciprocal-space representations of $|D_n(z)\rangle \in \mathcal{L}^2(\mathrm{R})$. The vacuum wavevectors $\mathbf{K}_O$ and $\mathbf{K}_G = \mathbf{K}_O + \mathbf{g}_0$ are tuned to kinematical resonance, *i.e.* they satisfy Bragg's law $2\mathbf{g}_0\mathbf{K}_{OG} = \mp g_0^2$, $K = K_O = K_G$ is the X-ray wavenumber in vacuum, Θ is the Bragg angle and $\kappa = \chi_o K/(2\cos\Theta_B)$. It is to be noted that the choice of $\mathbf{g}_0$ and, consequently, of $\mathbf{K}_O$ and $\mathbf{K}_G$ is not unique. In other words, the same physics can be described by different choices of $\mathbf{g}_0$ and, consequently, of deformation.

The master equations for the X-ray dynamics in deformed crystals are to be found in a previous article [equations (36) and (46) in Mana & Montanari (2004)]. Our present starting point is the reciprocal-space representation of Takagi's equations for a semi-infinite deformed crystal,

$$\begin{aligned} p_z\overline{D}_O &= -q\overline{D}_O\tan\Theta_B + K\overline{\chi}^u_{\bar{g}} * \overline{D}_G/(2\cos\Theta_B) \\ p_z\overline{D}_G &= K\overline{\chi}^u_g * \overline{D}_O/(2\cos\Theta_B) + q\overline{D}_G\tan\Theta_B, \end{aligned} \tag{5}$$

which, in the direct space, read

$$\mathrm{i}\partial_z\begin{bmatrix} D_O \\ D_G \end{bmatrix} = \begin{bmatrix} -\mathrm{i}\tan\Theta_B\partial_x & \nu\exp(-\mathrm{i}\mathbf{g}_0\mathbf{u}) \\ \nu\exp(+\mathrm{i}\mathbf{g}_0\mathbf{u}) & \mathrm{i}\tan\Theta_B\partial_x \end{bmatrix}\begin{bmatrix} D_O \\ D_G \end{bmatrix}. \tag{6}$$

In the above equations, the resonance error, $\mathbf{p} = p_z\hat{\mathbf{z}} + q\hat{\mathbf{x}}$, is split into one component orthogonal to the observation plane, p_z, and one, q, in the observation plane, and $\nu = \hat{\mathbf{e}}_O\hat{\mathbf{e}}_G\chi_{\pm g}K/(2\cos\Theta_B)$ is a coupling constant. The Fourier components of electric susceptibility $\chi^u_{\pm g}(\mathbf{r}) = \hat{\mathbf{e}}_O\hat{\mathbf{e}}_G\chi_{\pm g}\exp(\pm\mathrm{i}\mathbf{g}_0\mathbf{u})$ include the polarization factor, $\overline{\chi}^u_{\pm g}(\mathbf{p})$ is the Fourier transform of $\chi^u_{\pm g}(\mathbf{r})$, and $\overline{\chi}^u_{\pm g} * \overline{D}_{OG}$ are convolution integrals. In the following, p_z – the equivalent to energy in quantum mechanics – is called resonance error, q – the equivalent to linear momentum – is called the deviation parameter and, in addition to the Fourier transform

$$\overline{D}_n(q; p_z) = \int_{-\infty}^{+\infty} D_n(\mathbf{r})\exp(\mathrm{i}\mathbf{p}\mathbf{r})\,\mathrm{d}\mathbf{r}, \tag{7}$$

we shall use the mixed Fourier transform

$$\widetilde{D}_n(q; z) = \int_{-\infty}^{+\infty} D_n(x; z)\exp(\mathrm{i}qx)\,\mathrm{d}x. \tag{8}$$

The Hamiltonian operator $\mathbf{H}$ is so defined that $\langle x'|\mathbf{H}|x\rangle = \delta(x - x')H(x; z)$, where $H(x; z)$ is the 2×2 matrix in (6). As suggested by the convolutions, propagation modes are not plane-wave superpositions; interaction mixes states having different deviation parameters and, therefore, $\langle q'|\mathbf{H}|q\rangle = \widetilde{H}(q - q'; z)$. However, in a perfect crystal, propagation modes are plane-wave superpositions and, consequently, $\langle q'|\mathbf{H}_0|q\rangle = \delta(q - q')\widetilde{H}_0(q)$.

In the derivation of (5), we assumed that the variance of $\mathbf{p}$ in $\chi^u_{\pm g}$ is negligible when compared with g_0^2 [*cf.* equation (29) in Mana & Montanari (2004)]. In the direct space, the corresponding assumptions, $|\partial_{ij}u_g/g_0| \ll 1$ and $(\partial_i u_g)^2 \ll 1$, where $u_g = \hat{\mathbf{g}}_0\mathbf{u}$, are discussed by Authier (2001) and Härtwig (2001).

2.2. Eikonal representation

A way to solve (6) is to diagonalize the Hamiltonian operator by solving the related eigenvalue problem (Mana & Montanari, 2004). In a general case, this analytical integration is not possible, as the Hamiltonian eigenvectors move in the Hilbert space. A way to describe X-ray propagation is the elimination of this motion through an appropriate representation of the crystal field. According to this approach, it is still possible to define wavefields. The only difference from the perfect-crystal case is that they are no longer plane-wave superpositions; wavefield wavefronts bend, adjusting themselves to the deformation in such a way that Bragg's law is always locally satisfied.

Let us consider the basis plane waves propagating along the wavevectors $\mathbf{K}_o$ and $\mathbf{K}_g = \mathbf{K}_o + \mathbf{g}$, which satisfy Bragg's law $2\mathbf{g}\mathbf{K}_{og} = \mp g^2$, where $\mathbf{g} = \mathbf{g}_0 - \nabla(\mathbf{g}_0\mathbf{u})$ is the local reciprocal vector. If we write $\mathbf{K}_{og} = \mathbf{K}_{OG} + \nabla S_{og}$, the eikonal-like function S_o must satisfy the equation

$$\mathbf{g}_0\nabla S_o = \mathbf{K}_G\nabla(\mathbf{g}_0\mathbf{u}) \tag{9}$$

and S_g must be calculated according to $S_g = S_o - \mathbf{g}_0\mathbf{u}$. In (9), we have used the first-order approximations $\mathbf{g}\nabla S_o \approx \mathbf{g}_0\nabla S_o$ and $g^2 \approx g_0^2 - 2\mathbf{g}_0\nabla(\mathbf{g}_0\mathbf{u})$. Equation (9) does not identify $\mathbf{K}_o$ uniquely, since any S_o can be replaced by a new eikonal $S_o' = S_o + \varsigma$, where $\mathbf{g}_o\nabla\varsigma = 0$, without altering the kinematical resonance. In order to fix S_o uniquely, we require $K_o = K_g = K$, to which the additional constraint

$$\mathbf{K}_O\nabla S_o = 0 \tag{10}$$

will follow.

By application of (3), the state transformation

$$\begin{bmatrix} D_o \\ D_g \end{bmatrix} = \begin{bmatrix} \exp(\mathrm{i}S_o) & 0 \\ 0 & \exp(\mathrm{i}S_g) \end{bmatrix}\begin{bmatrix} D_O \\ D_G \end{bmatrix}, \tag{11}$$

that is,

$$\begin{aligned}\mathbf{D}(\mathbf{r}) = {} & [D_o(\mathbf{r})\exp[-\mathrm{i}(\mathbf{K}_O\mathbf{r} + S_o)]\hat{\mathbf{e}}_o \\ & + D_g(\mathbf{r})\exp[-\mathrm{i}(\mathbf{K}_G\mathbf{r} + S_g)]\hat{\mathbf{e}}_g]\exp(-\mathrm{i}\kappa z),\end{aligned} \tag{12}$$

leads to

$$\mathrm{i}\partial_z\begin{bmatrix} D_o \\ D_g \end{bmatrix} = \begin{bmatrix} -\mathrm{i}\tan\Theta_B\partial_x & \nu \\ \nu & \mathrm{i}\tan\Theta_B\partial_x \end{bmatrix}\begin{bmatrix} D_o \\ D_g \end{bmatrix}, \tag{13}$$

where we have used (10). Therefore, if a solution to (9) and to (10) exists, transformation (11) reduces the X-ray dynamics to propagation in a perfect crystal. From this point of view, transformation (11) removes the $\exp(-\mathrm{i}S_{og})$ terms from D_O and D_G and leaves D_o and D_g unaffected by deformation. However, propagation modes are now linear superpositions of the two modified plane waves $\exp[-\mathrm{i}(\mathbf{K}_{OG}\mathbf{r} + S_{og})]$ and energy flows along curved lines. As pointed out by Kato (Kato, 1973; Azaroff *et al.*, 1974, p. 407), equation (13), where $\tan\Theta_B$ substitutes for the speed of light and ν for the rest energy, is equivalent to Dirac's equation (in Hamiltonian form) in one dimension and in the absence of interactions. Since only one dimension is considered, only positive and negative energies need to be introduced and the spin concept is not relevant.

As can be verified by applying the $\hat{\mathbf{K}}_O\nabla$ operator on both sides of (9) – since $\hat{\mathbf{K}}_O\nabla$ is the derivative along the $\mathbf{K}_O$ direction – a necessary condition for solving (9) and (10) is

$$\cos\Theta_B\partial_z^2 u_g - \sin\Theta_B\partial_x^2 u_g = 0, \tag{14}$$

which equation was obtained by Kato (Kato, 1973; Azaroff *et al.*, 1974, p. 413). This means that, if we have a solution for (6) with a displacement $\mathbf{u}$, the same solution, apart from a phase factor, applies to all displacements $\mathbf{u} + \mathbf{u}'$, provided that $\mathbf{u}'$ satisfies (14). In fact, transformation (11), where S_o is obtained by using $\mathbf{u}'$ in (9), eliminates the contribution of $\mathbf{u}'$ to the X-ray dynamics. As we shall presently show, this result corresponds to gauge invariance in electrodynamics and (11) is the relevant gauge transformation. In a general case, equations (9) and (10) have no solution and, therefore, X-ray dynamics cannot be reduced to propagation in a perfect crystal. Although we can still use the eikonal representation, where S_o is a solution for (9) and $S_g = S_o - \mathbf{g}_0\mathbf{u}$, now $\mathbf{K}_O\nabla S_o \neq 0$. In this case, since $\mathbf{g}_0\nabla S_g = \mathbf{K}_O\nabla(\mathbf{g}_0\mathbf{u})$ and $\mathbf{K}_G\nabla S_g = \mathbf{K}_O\nabla S_o$, as can be verified from (9) and Bragg's law, Takagi's equations read

$$\mathrm{i}\partial_z\begin{bmatrix} D_o \\ D_g \end{bmatrix} = \begin{bmatrix} -\mathrm{i}\tan\Theta_B\partial_x - \alpha & \nu \\ \nu & \mathrm{i}\tan\Theta_B\partial_x - \alpha \end{bmatrix}\begin{bmatrix} D_o \\ D_g \end{bmatrix}, \tag{15}$$

where α, which is either

$$\alpha = \hat{\mathbf{K}}_O\nabla S_o/\cos\Theta_B = \partial_z S_o + \tan\Theta_B\partial_x S_o \tag{16}$$

or

$$\alpha = \hat{\mathbf{K}}_G\nabla S_g/\cos\Theta_B = \partial_z S_g - \tan\Theta_B\partial_x S_g, \tag{17}$$

plays the role of the interaction potential in quantum mechanics. In (15), the D_{og} amplitudes propagate along $\mathbf{K}_{og} = \mathbf{K}_{OG} + \nabla S_{og}$, thus satisfying Bragg's law. However, the wavenumber of the basis plane waves, $K_{og} \approx K + \alpha\cos\Theta_B$, is no longer the wavenumber in vacuum.

2.3. *o–g* representation

We now propose to obtain the transformation by which the $\exp(\pm\mathrm{i}\mathbf{g}_0\mathbf{u})$ terms are removed from the Hamiltonian matrix and (6) are written in the usual form (Authier, 2001). This is accomplished by setting $S_o = 0$ and $S_g = -\mathbf{g}_0\mathbf{u}$, which correspond to the representation of the crystal field

$$\begin{aligned}\mathbf{D}(\mathbf{r}) = {} & \{\varphi_o(\mathbf{r})\exp(-\mathrm{i}\mathbf{K}_O\mathbf{r})\hat{\mathbf{e}}_o + \varphi_g(\mathbf{r})\exp[-\mathrm{i}(\mathbf{K}_G\mathbf{r} - \mathbf{g}_0\mathbf{u})]\hat{\mathbf{e}}_g\} \\ & \times\exp(-\mathrm{i}\kappa z).\end{aligned} \tag{18}$$

By application of (3), (18) leads to

$$\mathrm{i}\partial_z\begin{bmatrix} \varphi_o \\ \varphi_g \end{bmatrix} = \begin{bmatrix} -\mathrm{i}\tan\Theta_B\partial_x & \nu \\ \nu & \mathrm{i}\tan\Theta_B\partial_x + \alpha_g \end{bmatrix}\begin{bmatrix} \varphi_o \\ \varphi_g \end{bmatrix}, \tag{19}$$

where the interaction potential is

$$\alpha_g = \hat{\mathbf{K}}_G\nabla(\mathbf{g}_0\mathbf{u})/\cos\Theta_B. \tag{20}$$

As is known [*cf.*, for example, Mana & Montanari (2004), equations (68) and (70)], α_g is proportional to the $\mathbf{K}_O$ deviation from the centre of the reflection domain. Therefore, the effective misalignment is $\theta_e = -\alpha_g/g_0$ (Authier, 2001, p. 362),

where we have used $g_0 = 2K \sin\Theta_B$. Crystal deformation can be eliminated if a change in representation is possible, which uses resonant basis plane waves. In the *o–g* representation, the basis plane waves propagate along $\mathbf{K}_o = \mathbf{K}_O$ and $\mathbf{K}_g = \nabla(\mathbf{K}_G\mathbf{r} - \mathbf{g}_0\mathbf{u}) = \mathbf{K}_O + \mathbf{g}$, which, unless $\mathbf{K}_G\nabla(\mathbf{g}_0\mathbf{u}) = 0$, do not satisfy Bragg's law. In fact,

$$g^2 + 2\mathbf{K}_O\mathbf{g} \approx -2\mathbf{K}_G\nabla(\mathbf{g}_0\mathbf{u}) = -2K\cos\Theta_B\alpha_g, \qquad (21)$$

where we used $\mathbf{g} = \mathbf{g}_0 - \nabla(\mathbf{g}_0\mathbf{u})$, $2\mathbf{K}_O\mathbf{g}_0 = -g_0^2$ and $g^2 \approx g_0^2 - 2\mathbf{g}_0\nabla(\mathbf{g}_0\mathbf{u})$. Equation (21) suggests another way to interpret α_g. According to it, the local kinematical resonance error of the basis plane waves is accounted for, but rotation and strain are not distinguished because both combine linearly. Therefore, apart from boundary conditions, a strained crystal appears rotated to X-rays and *vice versa*. Additionally, since α_g depends only on the deformation component along $\mathbf{g}_0$, any deformation for which $\mathbf{K}_G\nabla(\mathbf{g}_0\mathbf{u}) = 0$ is inessential. It must be noted that the foregoing condition is equivalent to $\mathbf{K}_G\Delta\mathbf{g} = 0$, where $\Delta\mathbf{g} = \mathbf{g} - \mathbf{g}_0 = -\nabla(\mathbf{g}_0\mathbf{u})$ (Authier, 2001, p. 362). The vanishing of α_g does not mean that the solution of (6) is the same as that in a perfect crystal. In fact, although (19) reduces to perfect-crystal equations, the field amplitudes are different [*cf.* equations (48) and (49) in Mana & Montanari (2004)]. In the present case, the deformation is entirely singled out in the $\exp(\mathrm{i}\mathbf{g}_0\mathbf{u})$ phase factor, coherently with the observation that $\mathbf{K}_O$ and $\mathbf{g}$ satisfy Bragg's law.

We can also remove the $\exp(\pm\mathrm{i}\mathbf{g}_0\mathbf{u})$ terms from the Hamiltonian matrix symmetrically. To this end, let us set $S_o = \mathbf{g}_0\mathbf{u}/2$ and $S_g = -\mathbf{g}_0\mathbf{u}/2$; this corresponds to representing the crystal field by

$$\begin{aligned}\mathbf{D}(\mathbf{r}) = \{&\varphi_o(\mathbf{r})\exp[-\mathrm{i}(\mathbf{K}_O\mathbf{r} + \mathbf{g}_0\mathbf{u}/2)]\hat{\mathbf{e}}_o \\ &+ \varphi_g(\mathbf{r})\exp[-\mathrm{i}(\mathbf{K}_G\mathbf{r} - \mathbf{g}_0\mathbf{u}/2)]\hat{\mathbf{e}}_g\}\exp(-\mathrm{i}\kappa z). \qquad (22)\end{aligned}$$

By application of (3), (22) leads to

$$\mathrm{i}\partial_z\begin{bmatrix}\varphi_o\\ \varphi_g\end{bmatrix} = \begin{bmatrix}-\mathrm{i}\tan\Theta_B\partial_x - \alpha_o/2 & \nu\\ \nu & \mathrm{i}\tan\Theta_B\partial_x + \alpha_g/2\end{bmatrix}\begin{bmatrix}\varphi_o\\ \varphi_g\end{bmatrix}, \qquad (23)$$

where the interaction potential is

$$\alpha_{og} = \hat{\mathbf{K}}_{OG}\nabla(\mathbf{g}_0\mathbf{u})/\cos\Theta_B = g_0(\partial_z u_g \pm \tan\Theta_B\partial_x u_g). \qquad (24)$$

With correspondences $\mathrm{i}\partial_z + g_0\tan\Theta_B\partial_x u_g \rightarrow \mathrm{i}\partial_z + e\Phi$ and $\mathrm{i}\tan\Theta_B\partial_x + g_0\partial_z u_g \rightarrow \mathrm{i}\tan\Theta_B\partial_x - eA$, where e is the electron charge and Φ and A are the scalar and vector potential, (23) is equivalent to Dirac's equation in the presence of an electromagnetic field. Additionally, the potential components satisfy $\partial_x A + \partial_z\Phi/\tan\Theta_B = 0$, which is equivalent to the Coulomb gauge (Kato, 1973; Azaroff *et al.*, 1974, p. 407).

In (22), field amplitudes propagate along $\mathbf{K}_o = \mathbf{K}_O - \Delta\mathbf{g}/2$ and $\mathbf{K}_g = \mathbf{K}_G + \Delta\mathbf{g}/2 = \mathbf{K}_o + \mathbf{g}$. We investigate again the conditions under which $\mathbf{K}_o$ and $\mathbf{g}$ satisfy Bragg's law. By repeating the previous calculation, we obtain

$$g^2 + 2\mathbf{K}_o\mathbf{g} \approx (\mathbf{K}_O + \mathbf{K}_G)\nabla(\mathbf{g}_0\mathbf{u}). \qquad (25)$$

Therefore, Bragg's law is satisfied when $(\mathbf{K}_O + \mathbf{K}_G)\nabla(\mathbf{g}_0\mathbf{u}) = 0$, that is, when the u_g equipotential surfaces are orthogonal to $\mathbf{g}_0$.

3. Approximation methods

There are only few deformations for which Takagi's equations can be solved analytically. Numerical (Authier *et al.*, 1968; Epelboin, 1983; Carvalho & Epelboin, 1993; Epelboin, 1996) and approximation (Penning & Polder, 1961; Kato, 1963) methods therefore play an important role in the application of the theory. Presently, we shall outline some of the last, adapted from quantum mechanics.

3.1. Adiabatic approximation

When a deformation depends only on z, within the limit of an infinitely slow displacement, any initial eigenstate of $\mathbf{H}(0)$ will shift into the eigenstate of $\mathbf{H}(z)$ resulting from the former by continuity [adiabatic theorem, see Messiah (1962)]. Formally, the crystal-field propagator is

$$\mathbf{U}(z) = \mathbf{W}^{-1}(z)\exp\Big[-\mathrm{i}\int_0^z \mathbf{H}_\pm(t)\,\mathrm{d}t\Big]\mathbf{W}(0), \qquad (26)$$

where $\mathbf{H}_\pm = \mathbf{W}\mathbf{H}\mathbf{W}^{-1}$ is the diagonal representation of the Hamiltonian operator. According to (26), X-rays move inside the crystal tuning themselves to the local dispersion surface without interbranch transitions.

In order to exemplify this approximation, let the symmetrical *o–g* representation of the Hamiltonian be

$$\widetilde{H}(q) = \begin{bmatrix}-q_- & \nu\\ \nu & q_-\end{bmatrix}, \qquad (27)$$

where $q_-(z) = q\tan\Theta_B + \alpha_g(z)/2$ is the deviation parameter. The next step is to calculate the Hamiltonian eigenvalues, that is, the resonance errors,

$$p_z = p_\pm(q) = \pm\sqrt{q_-^2 + \nu^2}, \qquad (28)$$

and eigenstates, that is, the wavefields,

$$|q,\pm\rangle = \begin{bmatrix}q_- - p_\pm\\ -\nu\end{bmatrix}|q\rangle. \qquad (29)$$

The eigenvalues (28) define a two hyperbolic branch dispersion surface and completely determine the X-ray dynamics in perfect crystals (Mana & Montanari, 2004). The $|\pm\rangle \in \mathrm{c}^2$ states, characterized by positive or negative resonance errors, are the equivalent of positive and negative energy states of a spinless relativistic particle. We note that the perfect-crystal eigenvalues are degenerate, *e.g.* the wavefields $|-q,+\rangle$ and $|+q,+\rangle$ correspond to the same resonance error. With the $|q,\pm\rangle$ wavefields as a basis, the Hamiltonian

$$\widetilde{H}_\pm(q) = \begin{bmatrix}-\sqrt{q_-^2 + \nu^2} & 0\\ 0 & \sqrt{q_-^2 + \nu^2}\end{bmatrix} \qquad (30)$$

is diagonal. Eventually, the adiabatic approximation of the optical transfer matrix is

$$\widetilde{U}(q;z) = W^{-1}(z)\begin{bmatrix} \exp[\mathrm{i}S(z)] & 0 \\ 0 & \exp[-\mathrm{i}S(z)] \end{bmatrix} W(0), \quad (31)$$

where

$$S(z) = \int_0^z \sqrt{q_-^2 + \nu^2}\,\mathrm{d}t, \quad (32)$$

$$W = \frac{1}{2\nu\sqrt{q_-^2+\nu^2}}\begin{bmatrix} \nu & q_- - \sqrt{q_-^2+\nu^2} \\ -\nu & -q_- - \sqrt{q_-^2+\nu^2} \end{bmatrix} \quad (33)$$

and

$$W^{-1} = \begin{bmatrix} q_- + \sqrt{q_-^2+\nu^2} & q_- - \sqrt{q_-^2+\nu^2} \\ -\nu & -\nu \end{bmatrix}. \quad (34)$$

To examine the validity limits of (31), we observe that, according to (3), (31) corresponds to neglecting $W\partial_z W^{-1}$ when compared with $\widetilde{H}_\pm$. The largest eigenvalue, $\Lambda_e\partial_z q_-/(2\pi)$, of $W\partial_z W^{-1}$ must be compared with the smallest eigenvalue, π/Λ_e, of $\widetilde{H}_\pm$, where $\Lambda_e = \pi/\nu$ is the *Pendellösung* length. Since $2\partial_z q_- = \partial_z \alpha_g$, the validity condition for adiabatic approximation is

$$|\partial_z \alpha_g| \ll p_e^2, \quad (35)$$

where $p_e = 2\pi/|\Lambda_e|$, *i.e.* the gap between the positive and negative branches of the dispersion surface, is analogous to the Bohr frequency characterizing the transition between the $|q=0,+\rangle$ and $|q=0,-\rangle$ wavefields. Equation (35) indicates that the frequency of the $W\partial_z W^{-1}$ eigenstates must be low compared with the Bohr frequency of interbranch transition. When $\alpha_g = -g_0\theta_e$ is used, (35) reduces to the condition $|\partial_z\theta_e| \ll p_e\delta_0$ (Authier, 2001, p. 409), which indicates that the effective misalignment gradient must be smaller than the Darwin width $\delta_0 = p_e/g_0$ over a distance equal to the *Pendellösung* length.

3.2. Instantaneous approximation

We assume now the Hamiltonian to change from the initial value $\mathbf{H}_1$, at $z=0$, to the final value $\mathbf{H}_2$, at $z=T$. When T tends to zero, that is in the case of an infinitely rapid transition, the crystal field remains unchanged. This follows from the formal expression of the propagation operator

$$\mathbf{U}(T) = \exp\Big[-\mathrm{i}\int_0^T \mathbf{H}(t)\,\mathrm{d}t\Big] \approx \mathbf{I} - \mathrm{i}T\mathbf{H}_a, \quad (36)$$

where $\mathbf{I}$ is the identity operator; when T tends to zero, $\mathbf{U}(T)$ approximates the identity operator. The approximation error can be found by calculating the component of $\mathbf{U}(T)|1\rangle$ in the subspace orthogonal to the initial state $|1\rangle$, where $\langle 1|1\rangle = 1$. The relevant calculations we adapted from Messiah (1962) are given in Appendix *A*. The condition for the state modification to be negligible is $T \ll 1/\sigma_H$, where

$$\sigma_H^2 = \langle \mathbf{H}_a^\dagger \mathbf{H}_a\rangle - \langle \mathbf{H}_a\rangle^2 \quad (37)$$

is the variance of the average Hamiltonian

$$\mathbf{H}_a = (1/T)\int_0^T \mathbf{H}(t)\,\mathrm{d}t \quad (38)$$

in the initial state. In this case, a plane boundary can substitute for the transition region, the finite thickness of which is neglected.

3.3. Transfer-matrix expansion

We now review briefly the time-dependent perturbation theory. In quantum mechanics (Messiah, 1962; Fano, 1971), the Hamiltonian is assumed Hermitian, but this is not true in the case of Takagi's equations and, consequently, the theory extension must be examined with care. The perturbation method is based on the following manipulation of (15). In the first place, we split the Hamiltonian into two parts: $\mathbf{H}_0$, which describes a perfect crystal, and $\mathbf{V}$, which describes X-ray interaction with the deformation field. Hence, $\mathbf{H} = \mathbf{H}_0 + \mathbf{V}$, where $V(x;z) = -\alpha(x;z)I$, I being the 2×2 identity matrix. Then, we remove the perfect-crystal evolution of the crystal field by a change from the *o–g* representation to what is known as the interaction representation. Hence,

$$|D_I(z)\rangle = \mathbf{U}_0^{-1}(z)|D(z)\rangle = \exp(\mathrm{i}\mathbf{H}_0 z)|D(z)\rangle. \quad (39)$$

By application of (3), (39) leads to

$$\mathrm{i}\partial_z|D_I(z)\rangle = \mathbf{V}_I|D_I(z)\rangle, \quad (40)$$

where $\mathbf{V}_I = \mathbf{U}_0^{-1}\mathbf{V}\mathbf{U}_0$ is the interaction representation of $\mathbf{V}$ and $|D_I(0)\rangle = |D(0)\rangle$. The evolution of (39), $|D_I(z)\rangle = \mathbf{U}_I(z)|D(0)\rangle$, where

$$\mathbf{U}_I(z) = \mathbf{I} - \mathrm{i}\int_0^z \mathbf{V}_I(t)\mathbf{U}_I(t)\,\mathrm{d}t \approx \mathbf{I} - \mathrm{i}\int_0^z \mathbf{V}_I(t)\,\mathrm{d}t, \quad (41)$$

now takes place slowly, influenced by the deformation alone. Since $\mathbf{U}(z) = \mathbf{U}_0(z)\mathbf{U}_I(z)$, we obtain

$$\begin{aligned}\begin{bmatrix} \widetilde{D}_o(q;z) \\ \widetilde{D}_g(q;z) \end{bmatrix} \approx \widetilde{U}_0(q;z)\begin{bmatrix} \widetilde{D}_o(q;z) \\ \widetilde{D}_g(q;z) \end{bmatrix} \\ - \mathrm{i}\int_0^z \widetilde{U}_0(q;z-t)\int_{-\infty}^{+\infty}\widetilde{\alpha}(q-q',t)\widetilde{U}_0(q',t) \\ \times \begin{bmatrix} \widetilde{D}_o(q';0) \\ \widetilde{D}_g(q';0) \end{bmatrix}\mathrm{d}q'\,\mathrm{d}t. \end{aligned} \quad (42)$$

The usefulness of (42) depends on effective misalignment. The evolution operator $\mathbf{U}_I$ differs from identity in proportion to α; if it is small, the perturbation expansion converges rapidly and we only need to consider the first term (Fano, 1971, p. 366). Let us suppose that, initially, the field state is a perfect-crystal wavefield, say $|q_a, s_a\rangle$, where $s_a = \pm 1$ is the sign of the resonance error and $\langle q_a, s_a|q_a, s_a\rangle = 1$. We calculate $w_{ab}^2 = |\langle q_b, s_b|\mathbf{U}(z)|q_a, s_a\rangle|^2$, *i.e.* the scattered intensity density in a different wavefield, say $|q_b, s_b\rangle$, where $\langle q_b, s_b|q_b, s_b\rangle = 1$. Since $\mathbf{U}_0(z)|q,s\rangle = \exp(-\mathrm{i}p_s z)|q,s\rangle$, through (41), we get

$$w_{ab}^2 = \Big|\int_0^z \widetilde{V}_{ba}(q_{ba};t)\exp(\mathrm{i}p_{ba}t)\,\mathrm{d}t\Big|^2 \exp(2\mu_b z), \quad (43)$$

where

$$\widetilde{V}_{ba}(q_{ba};z)=c_{ba}\widetilde{\alpha}(q_{ba};z) \tag{44}$$

is the $\langle q_b,s_b|\alpha(z)|q_a,s_a\rangle$ matrix element relative to the transition, $c_{ba}(q_b,q_a)=\langle s_b|s_a\rangle$ is the amplitude of the initial resonance-error state, $|s_a\rangle\in \mathrm{c}^2$, in the final state, $|s_b\rangle\in \mathrm{c}^2$, $q_{ba}=q_b-q_a$ is the deviation parameter difference, $\mu_b=\mathrm{Im}(p_b)$ is the final wavefield absorption, $p_{ba}=p_{sb}(q_b)-p_{sa}(q_a)$ is the transition Bohr frequency, and $p_\pm(q)$ are the perfect-crystal resonance errors (28), where $q_-=q\tan\Theta_B$. It is to be noted that p_{ba} is complex, since $\mathbf{H}_0$ is not Hermitian.

The scattered intensity density (43) is proportional to the squared modulus of the p_{ba} component in the harmonic analysis of $\widetilde{V}_{ba}(q_{ba};z)$. This analysis is simple when α does not depend on z. Then

$$w_{ab}^2=\frac{4|c_{ba}\widetilde{\alpha}_{ba}(q_{ba})|^2\exp[(\mu_a+\mu_b)z]|\sin(p_{ba}z/2)|^2}{|p_{ba}|^2}. \tag{45}$$

For any given value of z, the scattered intensity depends on the transition Bohr frequency and has a peak at $p_{ba}=0$; scattering proceeds towards states situated in a resonance-error band of $2\pi/z$ width. The scattered intensity density is shown in Fig. 1. When $q_b=q_a$ and, consequently, $p_{ba}=0$, resonances appear. Fig. 1 also shows the intensity $|c_{ab}|^2$ of $|s_a\rangle$ in $|s_b\rangle$. When $q_b\to-\infty$, since the initial resonance-error state approximates $|o\rangle$ and the final state, too, approximates $|o\rangle$, $c_{ab}=1$. On the contrary, when $q_b\to+\infty$, the final state approximates $|h\rangle$ and $c_{ab}=0$. The resonance at $q_b=-q_a$ corresponds to the transition into the wavefield $|-q_a,+\rangle$. However, as shown by the $|c_{ab}|^2$ plot, in this case, the initial and final resonance-error states are quasi-orthogonal, so that this transition is practically impossible.

Analysis of the way the scattered intensity density depends on z requires calculation of the intensity,

$$w_{aa}^2=[1-\widetilde{\alpha}^2(0)z^2]\exp(2\mu_a z), \tag{46}$$

where $\mu_a=\mathrm{Im}(p_a)$, of the initial state as it propagates through the crystal. In (46), the exponential factor describes attenuation or amplification (Borrmann's effect), according to negative or positive resonance errors. But the crystal-field intensity is prevented from increasing by the $\exp(-\mathrm{i}\kappa z)$ factor in (18). If we observe that $2\lim_{z\to\infty}|\sin(p_{ba}z/2)|=\exp(|\mu_{ba}|z/2)$, for any given p_{ba} value, we notice that w_{ab}^2 oscillates with period $2\pi/\mathrm{Re}(p_{ba})$ and fades about the average value

$$\lim_{z\to\infty}\frac{w_{ab}}{w_{aa}}=\begin{cases}|c_{ba}\widetilde{\alpha}_{ba}(q_{ba})/p_{ba}|\exp(\mu_{ba}z) & \text{if } \mu_b>\mu_a\\ |c_{ba}\widetilde{\alpha}_{ba}(q_{ba})/p_{ba}| & \text{if } \mu_b<\mu_a.\end{cases} \tag{47}$$

For the above asymptotic relation to be valid, z must be large with respect to the oscillation period of (45) but, at the same time, be small for the first-order approximation (41) to be valid. According to (47), deformation produces an energy flow towards the states exhibiting the lowest absorption.

When α is a periodic function of z and has angular frequency $\wp$, with z much larger than $2\pi/\wp$ (Zolotoyabko & Panov, 1992), the scattered intensity density consists of two terms like (43), where $p_{ba}\pm\wp$ substitutes for p_{ba}. In practice, w_{ab} is everywhere small except in transitions having Bohr frequencies equal to $\pm\wp$. Therefore, if $\wp$ is low, only intrabranch scattering occurs and wavefields propagate adiabatically, but if $\wp$ is high, or the gap between the dispersion surface branches is low – which occurs for high X-ray energies, interbranch scattering occurs and new wavefields are excited on the opposite branch (Balibar *et al.*, 1975; Authier, 2001, p. 421).

It must be noted that Takagi's equations are obtained by a first-order approximation of resonance error (Mana & Montanari, 2004), which is reflected in the presence of only first-order derivatives in (6). Therefore, they correspond to the geometric approximation of visible optics, as can be verified by switching off the interaction with the crystal (Mana & Montanari, 2004). However, the coupling of the basis waves $|O\rangle$ and $|G\rangle$ with a definite wavevector closely imitates diffraction, understood as an interference between the plane-wave components of the field. When the spatial frequency of deformation is large enough for interbranch scattering to occur, deformation can be viewed as an obstacle in visible optics and as a source of secondary waves. The scattered

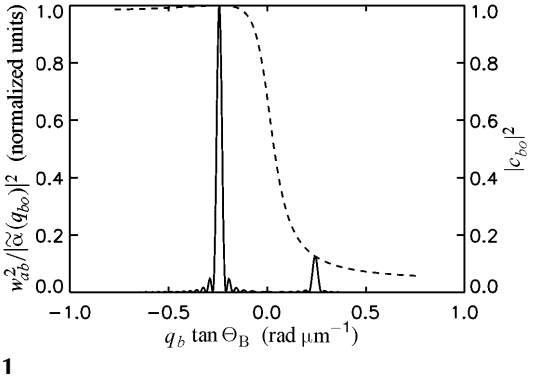

Figure 1
First-order intensity density (solid line) scattered from the $|q_a,+\rangle$ wavefield into the $|q_b,+\rangle$ wavefield (intrabranch scattering). Si (220) Laue symmetrical coplanar reflection, 17 keV X-rays, σ polarization, effective misalignment independent of z, $q_a=-1.25$ rad μm^{-1} and $z=200$ μm. When $q_b=\pm q_a$, resonances appear having widths inversely proportional to z. The broken line is the intensity $c_{ab}^2=|\langle s_b|s_a\rangle|^2$ of the initial resonance error state in the final state.

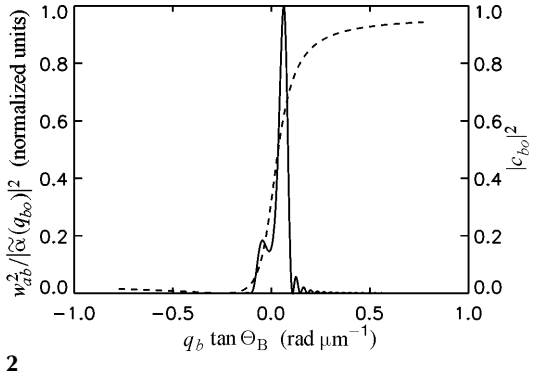

Figure 2
First-order intensity density (solid line) scattered from the $|q_a,+\rangle$ wavefield into the $|q_b,-\rangle$ wavefield (interbranch scattering). Si (220) Laue symmetrical coplanar reflection, 17 keV X-rays, σ polarization, periodic scattering potential having angular frequency $\wp=0.37$ rad μm^{-1}, $q_a=-1.25$ rad μm^{-1} and $z=200$ μm. When $q_b\approx0$ rad μm^{-1}, a resonance appears. The broken line is the intensity $c_{ab}^2=|\langle s_b|s_a\rangle|^2$ of the initial resonance error state in the final state.

intensity density is shown in Fig. 2; when $|q_b - q_a| = \wp$ resonance appears. In Fig. 2, the initial resonance-error state approximates $|o\rangle$. Therefore, when $q_b \to -\infty$, the final state, $|h\rangle$, is orthogonal to the initial state and $c_{ab} = 0$. On the contrary, when $q_b \to +\infty$, the final resonance-error state is the same $|o\rangle$ state and $c_{ab} = 1$. We note that interbranch transitions conserving the deviation parameter are impossible because the relevant initial and final resonance-error states are orthogonal and, consequently, $c_{ab} = 0$.

4. Deformation examples

In this section, we discuss some deformation examples. Two steps must be considered. Firstly, the matching of X-ray fields outside and inside a crystal and, secondly, the propagation of X-rays. Since outside the crystal $\mathbf{u} = 0$, the vacuum field is assumed to be represented in the *O–G* basis, that is, the D_{OG} field components are assumed to be input quantities. Since we shall describe field dynamics by means of the eikonal or the *o–g* representations, to specify the initial state we must apply a representation change.

4.1. Translation

Translation, $u_x = s = -u_g$, is a trivial deformation example. In this case, $\alpha_{og} = 0$, so that there is no effective potential and (23) is the equation of motion in a perfect crystal. Therefore, there is no wavefield change and X-rays behave as if no translation were present. However, the field amplitudes are different because the translation contribution to X-ray dynamics has been singled out in the $\exp(\mp i g_0 s/2)$ factor [*cf.* (22) and equation (48) in Mana & Montanari (2004)]. Therefore, the initial values of the crystal-field amplitudes are

$$D_{og}(x; 0) = \exp(\mp i g_0 s/2) D_{OG}(x; 0). \tag{48}$$

It is worth studying X-ray propagation also by the *O–G* representation. In this case, when we observe that $\chi^u_{\pm g} = \chi_{\pm g} \exp(\pm i g_0 s)$ are nothing else than the Fourier components of translated-crystal electrical susceptibility, (6) still corresponds to the equation of motion in perfect crystals and its solution [*cf.* equation (61) in Mana & Montanari (2004)] singles out the same $\exp(-i g_0 s)$ factor as (18) does.

4.2. Strain

The next deformation example is that of uniform strain. The $u_x = \varepsilon_0 x = -u_g$ deformation corresponds to diffracting planes uniformly strained by $\partial_x u_x = \varepsilon_0 \ll 1$. This deformation occurs when the wavevectors $\mathbf{K}_{OG}$ are tuned to kinematical resonance conditions with respect to a lattice parameter $\mathbf{g}_0 = -g_0 \hat{\mathbf{x}}$, which is different from the $\mathbf{g} = -(1 - \varepsilon_0) g_0 \hat{\mathbf{x}}$ lattice parameter. Consequently, if the eikonal representation is used, propagation in a perfect crystal will apply. Since $\mathbf{K}_{og} = K(\hat{\mathbf{z}} \cos\theta_B \pm \hat{\mathbf{x}} \sin\theta_B)$, $2K \sin\theta_B = (1 - \varepsilon_0) g_0 = 2(1 - \varepsilon_0) K \sin\Theta_B$, $\sin\theta_B = (1 - \varepsilon_0) \sin\Theta_B$ and $\cos\theta_B = (1 + \varepsilon_0 \tan^2\Theta_B) \cos\Theta_B$, we can write

$$\mathbf{K}_{og} = \mathbf{K}_{OG} + \kappa_\varepsilon \hat{\mathbf{z}} \mp q_\varepsilon \hat{\mathbf{x}}, \tag{49}$$

where $2q_\varepsilon = \varepsilon_0 g_0$, $2\kappa_\varepsilon = \varepsilon_0 g_0 \tan\Theta_B$.

We are now going to calculate the local wavevectors $\mathbf{K}_{og}$ by solving

$$\begin{aligned} \partial_x S_o &= -\mathbf{K}_G \nabla u_g = -\varepsilon_0 K \sin\Theta_B = -q_\varepsilon \\ \partial_z S_o &= -\tan\Theta_B \partial_x S_o = \kappa_\varepsilon. \end{aligned} \tag{50}$$

Hence,

$$S_{og}(x; z) = \kappa_\varepsilon z \mp q_\varepsilon x, \tag{51}$$

where we have used $S_g = S_o - g_0 u_g = S_o + 2q_\varepsilon x$. Finally, account being taken of $\mathbf{K}_{og} = \mathbf{K}_{OG} + \nabla S_{og}$, it is easy to obtain again (49). Additionally, since $\mathbf{g}_0 \mathbf{u} = -2q_\varepsilon x$, representations (12) and (22) are identical, apart from the $\kappa_\varepsilon z$ phase, which originates from (23) *via* $\alpha_{og} = \mp 2\kappa_\varepsilon$.

We must transform the initial state from the *O–G* representation into the *o–g* representation. Hence, $D_{og}(x; 0) = \exp(\mp i q_\varepsilon x) D_{OG}(x; 0)$ in the direct space, and $\widetilde{D}_{og}(q; 0) = \widetilde{D}_{OG}(q \mp q_\varepsilon; 0)$ in the reciprocal space. Finally, the X-ray dynamics is

$$\begin{bmatrix} \widetilde{D}_o(q; z) \\ \widetilde{D}_g(q; z) \end{bmatrix} = \widetilde{U}_0(q; z) \begin{bmatrix} \widetilde{D}_O(q - q_\varepsilon; 0) \\ \widetilde{D}_G(q + q_\varepsilon; 0) \end{bmatrix}. \tag{52}$$

Equation (52) can be obtained also through (18). To do so, we solve (19), where $\alpha_g = 2q_\varepsilon \tan\Theta_B$. The initial state is now

$$\begin{bmatrix} \varphi_o(x; 0) \\ \varphi_g(x; 0) \end{bmatrix} = \begin{bmatrix} D_O(x; 0) \\ D_G(x; 0) \exp(2i q_\varepsilon x) \end{bmatrix} \tag{53}$$

in the direct space and

$$\begin{bmatrix} \widetilde{\varphi}_o(q; 0) \\ \widetilde{\varphi}_g(q; 0) \end{bmatrix} = \begin{bmatrix} \widetilde{D}_O(q; 0) \\ \widetilde{D}_G(q + 2q_\varepsilon; 0) \end{bmatrix} \tag{54}$$

in the reciprocal space. Since α_g is a constant, X-ray propagation is (Mana & Montanari, 2004)

$$\begin{bmatrix} \widetilde{\varphi}_o(q; z) \\ \widetilde{\varphi}_g(q; z) \end{bmatrix} = \widetilde{U}_0(q + q_\varepsilon; z) \begin{bmatrix} \widetilde{D}_O(q; 0) \\ \widetilde{D}_G(q + 2q_\varepsilon; 0) \end{bmatrix} \exp(-i\kappa_\varepsilon z). \tag{55}$$

Account being taken of $D_n(x; z) = \exp[i(\kappa_\varepsilon z - q_\varepsilon x)] \varphi_n(x; z)$ and of $\widetilde{D}_n(q; z) = \widetilde{\varphi}_n(q - q_\varepsilon; z) \exp(i\kappa_\varepsilon z)$, we can prove that (55) is the same as (52).

4.3. Rotation

The last trivial example is that of uniform rotation. Hence, $u_x = \theta_0 z = -u_g$ and deformation corresponds to diffracting planes uniformly rotated by $\partial_z u_x = \theta_0 \ll 1$. This deformation occurs when a crystal is cut asymmetrically and the wavevectors $\mathbf{K}_{OG}$ are tuned to kinematical resonance with respect to a lattice parameter $\mathbf{g}_0 = -g_0 \hat{\mathbf{x}}$ different from $\mathbf{g} = -g_0(\hat{\mathbf{x}} - \theta_0 \hat{\mathbf{z}})$. By use of the eikonal representation, the wavevectors of the basis plane waves are $\mathbf{K}_{og} = K(\cos\psi_{og} \hat{\mathbf{z}} \pm \sin\psi_{og} \hat{\mathbf{x}})$, where $\psi_o = \Theta_B + \theta_0$ and $\psi_g = \Theta_B - \theta_0$. Since

$$\begin{aligned} \cos\psi_{og} &\approx \cos\Theta_B \mp \theta_0 \sin\Theta_B \\ \sin\psi_{og} &\approx \sin\Theta_B \pm \theta_0 \cos\Theta_B, \end{aligned} \tag{56}$$

we can also write

$$\mathbf{K}_{og} = \mathbf{K}_{OG} \mp \kappa_\theta \hat{\mathbf{z}} + q_\theta \hat{\mathbf{x}}, \tag{57}$$

where $2q_\theta = g_0\theta_0/\tan\Theta_B$ and $2\kappa_\theta = g_0\theta_0$. In order to demonstrate that $\mathbf{K}_{og} = \mathbf{K}_{OG} + \nabla S_{og}$ are the same wavevectors as in (57), we must solve

$$\begin{aligned} \partial_x S_o &= -\mathbf{K}_G \nabla u_g = \theta K \cos\Theta_B = q_\theta \\ \partial_z S_o &= -\tan\Theta_B \partial_x S_o = -\kappa_\theta. \end{aligned} \tag{58}$$

Hence,

$$S_{og}(x; z) = q_\theta x \mp \kappa_\theta z, \tag{59}$$

where $S_g = S_o + 2\kappa_\theta z$ has been used, and (57) follows immediately. Also in this case, since $\mathbf{g}_0\mathbf{u} = -2\kappa_\theta z$, (12) and (22) are identical, apart from the $q_\theta x$ phase, which originates from (23) *via* $\alpha_{og} = -2\kappa_\theta$. Eventually, the X-ray dynamics is

$$\begin{bmatrix} \widetilde{D}_o(q; z) \\ \widetilde{D}_g(q; z) \end{bmatrix} = \widetilde{U}_0(q; z) \begin{bmatrix} \widetilde{D}_O(q + q_\theta; 0) \\ \widetilde{D}_G(q + q_\theta; 0) \end{bmatrix}, \tag{60}$$

where the initial state is $D_{og}(x; 0) = \exp(\mathrm{i}q_\theta x) D_{OG}(x; 0)$ in the direct space and $\widetilde{D}_{og}(q; 0) = \widetilde{D}_{OG}(q + q_\theta; 0)$ in the reciprocal space.

We derive now (60) from (19), where $\alpha_g = -2q_\theta \tan\Theta_B$. Since α_g is a constant, X-ray propagation is (Mana & Montanari, 2004)

$$\begin{bmatrix} \widetilde{\varphi}_o(q; z) \\ \widetilde{\varphi}_g(q; z) \end{bmatrix} = \widetilde{U}_0(q - q_\theta; z) \begin{bmatrix} \widetilde{D}_O(q; 0) \\ \widetilde{D}_G(q; 0) \end{bmatrix} \exp(\mathrm{i}\kappa_\theta z), \tag{61}$$

where $\widetilde{\varphi}_{og}(q; 0) = \widetilde{D}_{OG}(q; 0)$ is the initial state. When observing that $D_{og}(x; z) = \exp[\mathrm{i}(q_\theta x - \kappa_\theta z)]\varphi_{og}(x; z)$ and that $\widetilde{D}_{og}(q; z) = \exp(-\mathrm{i}\kappa_\theta z)\widetilde{\varphi}(q + q_\theta; z)$, it can immediately be verified that (60) is the same as (61).

4.4. Reversal of effective misalignment

We now consider X-ray propagation when the effective misalignment is reversed. We assume that, before and after reversal, X-rays propagate in a perfect crystal and that misalignment changes from the initial value $-\theta_0$ to the final value θ_0 according to

$$\theta_e(z) = \begin{cases} -\theta_0 & \text{if } z \le z_1 \\ \theta_0[2(z - z_1)/T - 1] & \text{if } z_1 < z < z_2 \\ \theta_0 & \text{if } z \ge z_2, \end{cases} \tag{62}$$

where $T = z_2 - z_1$. The reciprocal-space symmetrical *o*–*g* representation of the Hamiltonian is given by (27), where $\alpha_g = -g_0\theta_e$. The perfect-crystal resonance errors corresponding to different diffracting-plane misalignments and $q = 0$ are plotted in Fig. 3. Each hyperbola corresponds to a well defined resonance error; when θ_e tends to plus or minus infinity, the corresponding wavefield tends toward the $|o\rangle = [1, 0]^T$ or $|g\rangle = [0, 1]^T$ states indicated in the figure. We assume the initial state to be the wavefield $|q = 0, -\rangle$ and misalignment to be sufficiently large to deviate the $|o\rangle$ and $|g\rangle$ states from kinematical resonance conditions and to decouple them. Therefore, the initial state is $|q = 0,\ g\rangle$ and propagates along the $\mathbf{K}_g$ direction.

We first consider instantaneous reversal. The calculation of σ_H can be performed along the same lines as given in Appendix *A*. Hence, if $T \ll |\Delta_e|/\pi$, the field state remains constant, whereas misalignment reverses and, once reversal is completed, the field still propagates along $\mathbf{K}_g$. However, the field state is now $|q = 0, +\rangle$, so that interbranch scattering occurs.

We now consider adiabatic reversal. During reversal, apart from a phase factor, the field state, which is always $|q = 0, -\rangle$, glides along the negative branch and the field will be in the $|q = 0, o\rangle$ state once misalignment is reversed. Therefore, in this case, once reversal is completed, X-rays propagate along $\mathbf{K}_o$.

4.5. Constant strain gradient

Takagi's equations for a deformed crystal in which the strain gradient is constant can be solved exactly (Petrashen, 1973; Chukhovskii, 1974; Katagawa & Kato, 1974; Litzman & Janacek, 1974; Authier, 2001, p. 410). We here illustrate an additional solution, which is based on Fourier optics and is valid for arbitrary waves falling on the crystal. The stated deformation

$$u_x = -u_g = a(x - s)(z - z_0) + s, \tag{63}$$

where (s, z_0) is the deformation origin, corresponds to a uniformly bent crystal, where the diffracting planes are rotated by $\theta(x) = \partial_z u_x = a(x - s)$ and strained by $\varepsilon(z) = \partial_x u_x = a(z - z_0)$. This deformation includes translation (when $a = 0$), strain (when $z_0 \to \infty$ and $a \to 0$ with $az_0 \to -\varepsilon_0$) and rotation (when $s \to \infty$ and $a \to 0$ with $as \to -\theta_0$). The local reciprocal vector of the deformed crystal is

$$\mathbf{g} = -g_0[(1 - \varepsilon)\hat{\mathbf{x}} - \theta\hat{\mathbf{z}}]. \tag{64}$$

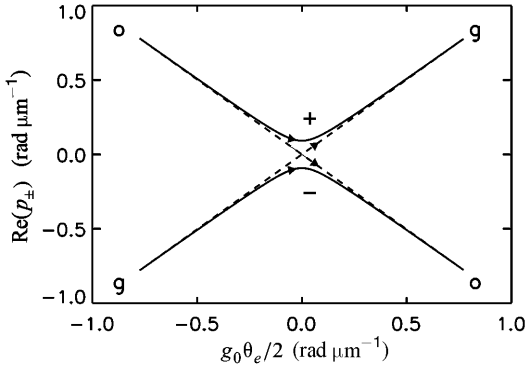

Figure 3
Projection of the perfect-crystal resonance error, $p_\pm(q = 0)$, in the $\mathrm{Im}(p_\pm) = 0$ plane as functions of effective misalignment, θ_e. Si (220) Laue symmetrical coplanar reflection, 17 keV X-rays and σ polarization. The asymptotic perfect-crystal wavefields when $\theta_e \to \pm\infty$ are indicated at the end of each hyperbola. Arbitrary field states, represented by points between the two hyperbolae, are linear wavefield superpositions with weights given by the distances from the relevant resonance error. Arrows indicate the evolution of the field state when the effective misalignment is reversed. The solid line indicates adiabatic reversal, the broken line instantaneous reversal.

By application of (24),

$$\alpha_{og} = -4\rho_x x' \tan\Theta_B \mp 4\rho_z z', \tag{65}$$

where $\rho_x = ag_0/(4\tan\Theta_B)$, $\rho_z = (ag_0/4)\tan\Theta_B$, $z' = z - z_0$ and $x' = x - s$, and the equations of motion for field amplitudes (22) are

$$(\mathrm{i}\partial_z - 2\rho_z z')\begin{bmatrix}\varphi_o\\ \varphi_g\end{bmatrix} = \begin{bmatrix}-(\mathrm{i}\partial_x - 2\rho_x x')\tan\Theta_B & \nu\\ \nu & (\mathrm{i}\partial_x - 2\rho_x x')\tan\Theta_B\end{bmatrix}\begin{bmatrix}\varphi_o\\ \varphi_g\end{bmatrix}. \tag{66}$$

In order to solve (66), we set

$$\varphi_{og} = D_{og}\exp[-\mathrm{i}(\rho_x x'^2 + \rho_z z'^2)], \tag{67}$$

so that (66), which now reads

$$\mathrm{i}\partial_z\begin{bmatrix}D_o\\ D_g\end{bmatrix} = \begin{bmatrix}-\mathrm{i}\tan\Theta_B\partial_x & \nu\\ \nu & \mathrm{i}\tan\Theta_B\partial_x\end{bmatrix}\begin{bmatrix}D_o\\ D_g\end{bmatrix}, \tag{68}$$

reduces to equations of motion in a perfect crystal.

We now examine X-ray propagation by using the eikonal representation. To this end, we must solve

$$\begin{aligned}\partial_x S_o &= -\mathbf{K}_G\nabla u_g = 2\rho_x(x' - z'\tan\Theta_B)\\ \partial_z S_o &= -\tan\Theta_B\partial_x S_o = 2\rho_z(z' - x'/\tan\Theta_B),\end{aligned} \tag{69}$$

where $u_g = -ax'z' - s$. The solutions of (69),

$$S_o(x; z) = \rho_x x'^2 + \rho_z z'^2 + g_0 u_g/2 \tag{70}$$

and

$$S_g(x; z) = \rho_x x'^2 + \rho_z z'^2 - g_0 u_g/2, \tag{71}$$

justify the use of the D_{og} symbols to indicate field amplitudes in (67). In order to prove explicitly that the $\exp[-\mathrm{i}(\mathbf{K}_{OG}\mathbf{r} + S_{og})]$ plane waves track crystal deformation, let us observe that, as the x coordinate varies, the wavefront bends and the deviation from Bragg's angle,

$$\vartheta_g(x; z) = \frac{\partial_x S_g(x; z)}{K\cos\Theta_B} = a(x' + z'\tan\Theta_B), \tag{72}$$

is equal to the effective misalignment

$$\theta_e(x; z) = -\frac{\partial_g u_g}{\cos\Theta_B} = a(x' + z'\tan\Theta_B). \tag{73}$$

To complete the analysis of X-ray propagation, we must fix the initial state at $z = 0$. To this end, in the first place, we write

$$g_0 u_g(x, 0) = -\varepsilon_0 g_0 x - g_1 s, \tag{74}$$

where $g_1 = g_0(1 - \varepsilon_0)$ is the magnitude of $\mathbf{g}(x, 0)$ and $\varepsilon_0 = -az_0$ is the diffracting-plane strain at $z = 0$. In the second place, apart from an inessential phase term common to both the o and g components, we write

$$D_{og}(x; 0) = D_{OG}(x; 0)\exp(\mathrm{i}\rho_x x^2)\exp(\mathrm{i}q_{og}x)\exp(\mp\mathrm{i}g_1 s/2), \tag{75}$$

where

$$2q_{og} = 2(q_\theta \mp q_\varepsilon) = (\theta_0/\tan\Theta_B \mp \varepsilon_0)g_o \tag{76}$$

and $\theta_0 = -as$ and $\varepsilon_0 = -az_0$ are the local diffracting-plane rotation and strain at the reference frame origin. In the third last place, the initial state is

$$\widetilde{D}_{og}(q; 0) = [\widetilde{D}_{OG} * \widetilde{F}](q + q_{og})\exp(\mp\mathrm{i}g_1 s/2), \tag{77}$$

where

$$\widetilde{F}(q) = \mathrm{i}\sqrt{\pi/2}\exp(-\mathrm{i}q^2/4\rho_x) \tag{78}$$

is the Fourier transform of $\exp(\mathrm{i}\rho_x x^2)$. Finally, the solution of Takagi's equation for a crystal with a constant strain gradient is

$$\begin{bmatrix}\widetilde{D}_o(q; z)\\ \widetilde{D}_g(q; z)\end{bmatrix} = \widetilde{U}_0(q; z)\begin{bmatrix}\widetilde{D}_o(q; 0)\\ \widetilde{D}_g(q; 0)\end{bmatrix}, \tag{79}$$

where $\widetilde{U}_0(q; z)$ is given by the dynamical theory of X-ray diffraction in perfect crystals (*e.g.* Mana & Montanari, 2004), D_{og} are given by (12), and S_{og} are given by (70) and (71). In the direct space, the searched solution is obtained by back-transforming (79). A detailed examination of the solution and wavefields properties can be found in the copious literature (*e.g.* Authier, 2001, p. 375). We only observe that, in (75), the first phase term expresses the lens effect of the bent crystal, the second the effective diffracting-plane rotation, and the third the differential phase shift between the o and g components.

5. Discussion of results

Equation (77) is a key result in the application of X-ray diffraction to the absolute measurement of the Si lattice parameter by X-ray interferometry. The interferometer consists of three plane-parallel Si crystals, which split and recombine X-rays by successive symmetrical Laue diffractions (Bonse & Hart, 1965). When the third crystal, the analyser, is moved orthogonally to the diffracting planes, periodic intensity variations in the emerging forward-diffracted and deviated X-rays occur, whose period, in the case of a geometrically perfect crystal (Mana & Vittone, 1997*a*,*b*), is equal to the diffracting-plane spacing. The analyser recombines the vacuum-field amplitudes D_O and D_G and, according to (48), X-ray fringes are originated by the $g_0 s$ phase shift between the D_o and D_g crystal-field amplitudes. In the case of a deformed analyser, matching between the vacuum- and crystal-field amplitudes is described by (77). Therefore, the phase shift is now $g_1 s$ and the fringe period is equal to the diffracting-plane spacing on the analyser surface. This result is somewhat surprising and we verified it by a numerical simulation (Mana *et al.*, 2004*a*). The usual description of the interferometer operation (*cf.*, for example, Bonse & Hart, 1965; Authier, 2001, p. 483) traces the travelling X-ray fringes back to the aligned or anti-aligned diffracting-plane position with respect to the nodes of the standing wave generated inside the analyser. Therefore, the concept of average diffracting-plane spacing seems the most important. On the contrary, our revisited theory ascribes X-ray fringes mostly to

boundary conditions, which includes both the vacuum-field amplitude and deformation values at the analyser surface. We assert that, after the propagation modes and the phase shifts between the D_o and D_g amplitudes have been set at the boundary, X-rays are delivered through the analyser adiabatically, without any further differential phase retardation between the D_{og} interfering amplitudes, which could depend on the analyser motion.

Equation (77) plays a key role also in a precise comparison of two Si-crystal lattice parameters by double-crystal Laue spectrometry. A two-crystal spectrometer consists of two X-ray sources, two plane-parallel crystals and two detectors recording the rocking curves of successive Laue reflections (Hart, 1969). If both crystals have the same diffracting-plane spacing, then both detectors simultaneously record a peak when the diffracting planes of the two crystals are precisely parallel. On the contrary, if diffracting-plane spacings are different, the two rocking curves peak at different angles. The equation for the difference in diffracting-plane spacings can be obtained from (76). When θ_0 is the Bragg rotation of the second crystal relative to the first, the peak separation is $\Delta\theta = 2\varepsilon_0 \tan\Theta_B$. Since $\varepsilon_0 g_0 = g_0 - g_1$, the measurement equation is

$$\frac{g_0 - g_1}{g_0} = \frac{\Delta\theta}{2\tan\Theta_B}. \tag{80}$$

Also in this case, contrary to what we expected, the inferred difference refers to the crystal surface. In order to verify also this result, a numerical simulation, *ab initio*, of the two-crystal spectrometer is under way (Mana *et al.*, 2004*b*).

6. Conclusions

We completed a reformulation of the dynamical theory of X-ray diffraction based on Fourier optics and on the analogy, first suggested by Kato (1973) and further developed by Mana & Montanari (2004), between Takagi's and Dirac's equations. This approach provides new insights into various aspects of the dynamical theory. A first example is the interpretation of *Pendellösung* fringes as the counterpart of quantum beats in fluorescence after coherent excitation of two close levels. Another example is the interpretation of interbranch scattering as the counterpart of induced transitions between energy levels. In the same way as occurs with quantum systems, when the crystal lattice does not vary adiabatically, each perfect-crystal wavefield diffuses into the other, with scattering proportional to the amplitude of the effective misalignment spectrum component at the Bohr frequency of the transition. The last example is the validity analysis, based on the instantaneous approximation of the vacuum-to-crystal transition, of substituting a mathematical plane for the crystal surface. We have also given a new solution of Takagi's equation for a crystal with a constant strain gradient, on the basis of Fourier optics and for any initial vacuum field. Finally, we demonstrated that the apparent fringe period and rocking-curve shift, that is, the values of diffracting-plane spacing measured by X-ray interferometry and two-crystal spectrometry, are equal to the diffracting-plane spacing on the crystal surface.

APPENDIX *A*
Validity limits of instantaneous approximation

Our derivation of the validity limits of instantaneousness follows that of Messiah (1962), which we think advisable to outline here to get to the roots of his result, before considering an exemplifying case. An estimate of the approximation error is component $w^2 = \langle 2|\mathbf{Q}^\dagger\mathbf{Q}|2\rangle$ of the final field state $|2\rangle = \mathbf{U}|1\rangle$ in the subspace orthogonal to the initial field state $|1\rangle$. Since the projection $\mathbf{Q} = \mathbf{I} - |1\rangle\langle 1|$ is idempotent, that is, $\mathbf{Q}^\dagger\mathbf{Q} = \mathbf{Q}$, and since the propagator can be approximated by $\mathbf{U} \approx (\mathbf{I} - \mathrm{i}T\mathbf{H}_a)$, where $\mathbf{H}_a$ is defined in (38), the required component is

$$\begin{aligned} w^2 &= \langle 1|(\mathbf{I} + \mathrm{i}T\mathbf{H}_a^\dagger)\mathbf{Q}(\mathbf{I} - \mathrm{i}T\mathbf{H}_a)|1\rangle \\ &= T^2\langle 1|\mathbf{H}_a^\dagger\mathbf{Q}\mathbf{H}_a|1\rangle + \mathrm{i}T\langle 1|(\mathbf{H}_a^\dagger\mathbf{Q} - \mathbf{Q}\mathbf{H}_a)|1\rangle, \end{aligned} \tag{81}$$

in which we assumed that the initial and final states are unit vectors. Since

$$\begin{aligned} \langle 1|\mathbf{H}_a^\dagger\mathbf{Q}\mathbf{H}_a|1\rangle &= \langle 1|\mathbf{H}_a^\dagger\big(\mathbf{I} - |1\rangle\langle 1|\big)\mathbf{H}_a|1\rangle \\ &= \langle 1|\mathbf{H}_a^\dagger\mathbf{H}_a|1\rangle - \langle 1|\mathbf{H}_a|1\rangle^2 = \sigma_H^2 \qquad (82) \\ \langle 1|\mathbf{Q}\mathbf{H}_a|1\rangle &= \langle 1|\big(\mathbf{I} - |1\rangle\langle 1|\big)\mathbf{H}_a|1\rangle = 0 \qquad (83) \end{aligned}$$

and, similarly, $\langle 1|\mathbf{H}_a^\dagger\mathbf{Q}|1\rangle = 0$, we can rewrite the approximation error as $\sigma_H T$, which must be negligible with respect to the initial-state norm $\langle 1|1\rangle$.

In order to give an example of the practical use of this result, we study the transition from vacuum to crystal propagation. Let us consider a coplanar symmetrical Laue geometry, the x axis being directed along $-\mathbf{g}_0$, and let $\langle q|\mathbf{H}|q'\rangle = \delta(q - q')\widetilde{H}(q; z)$, where

$$\widetilde{H}(q; z) = \begin{bmatrix} -q\tan\Theta_B & \nu f(z) \\ \nu f(z) & q\tan\Theta_B \end{bmatrix}; \tag{84}$$

let us also take the crystal boundary into account by setting

$$f(z) = \begin{cases} 0 & \text{if } z \le 0 \\ z/T & \text{if } 0 < z < T \\ 1 & \text{if } z \ge T. \end{cases} \tag{85}$$

The average Hamiltonian across the boundary, $\widetilde{H}_a(q)$, is still given by (84), where 1/2 substitutes for $f(z)$. Let the wavepacket $\mathbf{D}^{\mathrm{in}}(\mathbf{r})$ propagating along the $\mathbf{K}_O$ direction be the initial field. Hence,

$$\langle q|1\rangle = \widetilde{D}^{\mathrm{in}}(q; 0)\begin{bmatrix} 1 \\ 0 \end{bmatrix}, \tag{86}$$

where $\langle 1|1\rangle = \int_{-\infty}^{+\infty} \big|\widetilde{D}^{\mathrm{in}}(q; 0)\big|^2\,\mathrm{d}q/(2\pi) = 1$,

$$\langle 1|\mathbf{H}_a|1\rangle = -\frac{1}{2\pi}\int_{-\infty}^{+\infty} q\big|\widetilde{D}^{\mathrm{in}}(q; 0)\big|^2\tan\Theta_B\,\mathrm{d}q = -\langle q\rangle\tan\Theta_B, \tag{87}$$

where $\langle q\rangle$ is the expected value of q in the initial state, and

$$\langle 1|\mathbf{H}_a^\dagger \mathbf{H}_a|1\rangle = \frac{1}{2\pi}\int_{-\infty}^{+\infty} \begin{bmatrix} -q\tan\Theta_B & \nu^*/2 \end{bmatrix} \begin{bmatrix} -q\tan\Theta_B \\ \nu/2 \end{bmatrix} \times |D^{\rm in}(q;0)|^2\,{\rm d}q$$
$$= \frac{1}{2\pi}\int_{-\infty}^{+\infty} (q^2\tan^2\Theta_B + |\nu|^2/4)\left|\widetilde{D}^{\rm in}(q;0)\right|^2 {\rm d}q$$
$$= |\nu|^2/4 + \langle q^2\rangle \tan^2\Theta_B, \quad (88)$$

where $\langle q^2\rangle$ is the second moment of q in the initial state. Thus, the variance of the mean Hamiltonian in the initial state is

$$\sigma_H^2 = \langle 1|\mathbf{H}_a^\dagger \mathbf{H}_a|1\rangle - \langle 1|\mathbf{H}_a|1\rangle^2 = |\nu|^2/4 + \sigma_q^2\tan^2\Theta_B, \quad (89)$$

where $\sigma_q^2 = \langle q^2\rangle - \langle q\rangle^2$ is the variance of q in the initial state. By using the Heisenberg uncertainty relation $\sigma_x\sigma_q \geq 1/2$ (where σ_x is the standard deviation of x in the initial state) and $|\nu| \approx \pi/|\Lambda_e|$ (where Λ_e is the *Pendellösung* length), if

$$\left(\frac{\pi^2}{4|\Lambda_e|^2} + \frac{\tan^2\Theta_B}{4\sigma_x^2}\right)T^2 \ll 1, \quad (90)$$

the validity condition of the instantaneous approximation $T\sigma_H \ll 1$ is satisfied and a mathematical surface can substitute for the real surface. In the case of the second term on the left-hand side of (90) being neglected, the validity condition simplifies to $T \ll |\Lambda_e|/2$. Thus, Laue's assumption of considering the crystal surface a mathematical plane, an assumption not so obvious for X-rays, can be viewed as a consequence of the mathematical structure of the theory.

APPENDIX *B*
List of the main symbols

$\mathbf{K}$	Wavevector of a generic plane wave *in vacuo*
$\mathbf{K}_{OG}$	Wavevectors of basis plane waves
$\mathbf{K}_{og} = \mathbf{K}_{OG} + \nabla S_{og}$	Wavevectors of basis plane waves
$\mathbf{k}$	Wavevector of a generic plane wave in crystals
$\mathbf{k}_{OG} = \mathbf{K}_{OG} + \kappa\hat{\mathbf{z}}$	Wavevectors of basis plane waves in crystals
$\kappa = \chi_o K/(2\cos\Theta_B)$	$\mathbf{k}_O$ component normal to the crystal surface
$\hat{\mathbf{z}}$	Normal to the crystal surface
Θ_B	Bragg's angle
$\mathbf{p} = q\hat{\mathbf{x}} + p_z\hat{\mathbf{z}}$	Resonance error
$p_\pm(q)$	Perfect-crystal Hamiltonian eigenvalue (resonance error in this paper)
q	Deviation parameter
$\mathbf{g}_0$	Reciprocal vector of unstrained diffracting planes
$\mathbf{u}$	Crystal deformation
$\mathbf{g} = \mathbf{g}_0 - \nabla(\mathbf{g}_0\mathbf{u})$	Reciprocal vector of strained diffracting planes
$\nu = \dfrac{\hat{\mathbf{e}}_O\hat{\mathbf{e}}_G\chi_{\mp g}K}{2\cos\Theta_B}$	Coupling coefficient
α, α_{og}	Interaction potential (eikonal and *o*–*g* representations)
$\theta_e = -\alpha_g/g_0$	Effective misalignment (symmetric coplanar geometry)
$\theta = \partial_z u_x$	Diffracting-plane rotation
$\varepsilon = \partial_x u_x$	Diffracting-plane strain
$q_\varepsilon = \varepsilon_0 g_0/2$	Shift of field components (strain, reciprocal space)
$q_\theta = \theta_0 g_0/(2\tan\Theta_B)$	Shift of the field components (rotation, reciprocal space)
$q_{og} = q_\theta \mp q_\varepsilon$	Shift of field components (constant strain gradient, reciprocal space)
D_{OG}, D_{og}, φ_{og}	Field components (direct space, *O*–*G* eikonal and *o*–*g* representations)
$\mathbf{H}$	Deformed-crystal Hamiltonian
$\mathbf{H}_0$	Perfect-crystal Hamiltonian
$\widetilde{H}(q;z)$	Reciprocal-space representation of $\mathbf{H}$
$H(x;z)$	Direct-space representation of $\mathbf{H}$
$\widetilde{H}_\pm(q;z)$	Reciprocal-space diagonal representation of $\mathbf{H}$
$\|q;\pm\rangle$	Perfect-crystal Hamiltonian eigenvector
$\mathbf{U}$	Propagation operator
$\widetilde{U}_0(q;z)$	Perfect-crystal transfer matrix

This work was carried out in the framework of a research cooperation of the Consultative Committee for Mass and Related Quantities of the International Committee for Weights and Measures to determine the Avogadro constant with a target relative uncertainty of 2×10^{-8}.

References

Authier, A. (2001). *Dynamical Theory of X-ray Diffraction.* IUCr/Oxford University Press. Revised paperback edition 2003.

Authier, A., Malgrange, C. & Tournarie, M. (1968). *Acta Cryst.* A**24**, 126–136.

Azaroff, L. V., Kaplow, R., Kato, N., Weiss, R. D., Wilson, A. J. C. & Young, R. A. (1974). *X-ray Diffraction.* New York: McGraw Hill.

Balibar, F., Epelboin, Y. & Malgrange, C. (1975). *Acta Cryst.* A**31**, 836–840.

Bergamin, A., Cavagnero, G., Mana, G. & Zosi, G. (1999). *Eur. Phys. J.* **9**, 225–232.

Bonse, U. & Hart, M. (1965). *Appl. Phys. Lett.* **6**, 155–156.

Carvalho, C. A. M. & Epelboin, Y. (1993). *Acta Cryst.* A**49**, 460–467.

Chukhovskii, F. N. (1974). *Kristallografiya*, **19**, 482–488.

Deslattes, R. D., Kessler, E. G., Owens, S., Black, D. & Henins, A. (1999). *J. Phys. D*, **32**, A3–A7.

Epelboin, Y. (1983). *Acta Cryst.* A**39**, 761–767.

Epelboin, Y. (1996). *J. Appl. Cryst.* **29**, 331–340.

Ewald, P. (1965). *Rev. Mod. Phys.* **37**, 46–56.

Fano, G. (1971). *Mathematical Methods of Quantum Mechanics.* New York: McGraw Hill.

Hart, M. (1969). *Proc. R. Soc. London Ser. A*, **309**, 281–297.

Härtwig, J. (2001). *J. Phys. D*, **34**, A70–A77.

Katagawa, T. & Kato, N. (1974). *Acta Cryst.* A**30**, 830–836.

Kato, N. (1963). *Acta Cryst.* **16**, 282–290.

Kato, N. (1973). *Z. Naturforsch. Teil A*, **28**, 604–609.

Kessler, E. G., Henins, A., Nielsen, L. & Arif, M. (1994). *J. Res. Natl Inst. Stand. Technol.* **99**, 1–18.

Kessler, E. G., Owens, S. M., Henins, A. & Deslattes, R. D. (1999). *IEEE Trans. Instrum. Meas.* **48**, 221–224.

Litzman, O. & Janacek, Z. (1974). *Phys. Status Solidi A*, **25**, 663–666.

Mana, G. & Montanari, F. (2004). *Acta Cryst.* A**60**, 40–50.

Mana, G., Palmisano, C. & Zosi, G. (2004*a*). *Metrologia*. To be published.

Mana, G., Palmisano, C. & Zosi, G. (2004*b*). Submitted to *IEEE Trans. Instrum. Meas.* special issue on selected papers of CPEM/04, London, 27 June–2 July 2004.

Mana, G. & Vittone, E. (1997*a*). *Z. Phys.* B**102**, 189–196.

Mana, G. & Vittone, E. (1997*b*). *Z. Phys.* B**102**, 197–206.

Messiah, A. (1962). *Quantum Mechanics*. Amsterdam: North-Holland.

Penning, P. & Polder, D. (1961). *Philips Res. Rep.* **16**, 419–440.

Petrashen, P. V. (1973). *Fiz. Tverd. Tela*, **15**, 3131–3132.

Shevchenko, M. B. & Pobydaylo, O. V. (2003). *Acta Cryst.* A**59**, 45–47.

Zolotoyabko, E. & Panov, V. (1992). *Acta Cryst.* A**48**, 225–231.